

# A GENERIC PEST SUBMODEL FOR USE IN INTEGRATED ASSESSMENT MODELS

L. Rasche, R. A. J. Taylor

**ABSTRACT.** *The sustainability of agricultural land use has been the subject of integrated assessments for some time. In these assessments, knowledge of various disciplines is combined to assess, e.g., the drawbacks and benefits of new agro-technologies, changes in management systems, and the introduction or abolition of agricultural policies. Crop models are often used in these assessments, and the more details the models can provide, the more factors can be considered. For example, the crop model EPIC can determine fertilizer and irrigation water use based on crop demand. However, pesticides can only be applied manually and have no impact on the crop. We therefore developed a pest submodel providing estimates of pesticide consumption based on pest pressure and the corresponding reactions of crops, thus completing a process loop analogous to the application of fertilizers or irrigation water. We distinguish three pest categories: insects, fungi, and weeds. For insects, a biological temperature response function is used to model the daily feeding rate, from which population growth is derived. Insect mortality is dependent on temperature and nutrient availability. Fungal disease spread depends on coefficients of primary and secondary infection, abundance of spores, and host density. The number of spores increases depending on a humidity and temperature function and decreases according to a decay rate. Crop stress is dependent on the ratio of healthy to infected plant tissue. Weeds are grown in EPIC the same way as crops and compete for the same resources. Herbicide applications are triggered when a specified ratio of weed to crop LAI is reached. Pesticide-induced mortality is modeled as a pesticide-specific dose-response curve. We tested the submodel by simulating five crops with the highest use of pesticides in the U.S. (cotton, maize, potatoes, soybeans, and wheat). Among other findings, the mean simulated application rates approached the reported mean application rates, and the spatial distributions of simulated and reported application rates matched well. We conclude that the new pest submodel is appropriate to estimate pesticide use on larger scales and can be employed to enhance integrated assessments.*

**Keywords.** *Crop modeling, EPIC, Fungal diseases, Insect pests, Pesticides, Weeds.*

Agriculture is essential for providing food, fiber, and biofuels. A growing population, rising incomes, a higher demand for renewable energy, effects of climate change, and other factors continuously put pressure on the agricultural sector to expand and intensify its production. Simultaneously, the agricultural sector is expected to evolve into a more sustainable system and minimize its negative effects on the environment (Foley et al., 2011). Balancing these demands is difficult and requires sophisticated methods capable of assessing the drawbacks and benefits of new agro-technologies, changes in management systems, and the introduction or abolition of agricultural policies (van Ittersum and Wery, 2007). Integrated assessments of agricultural land use are often employed for this task. These integrated assessments answer the question of how the benefits of agriculture can best be max-

imized while the environmental costs are minimized. For example, optimized pest management will be highly important in future, but its contribution to higher yields and prolonged food preservation has to be balanced against its external costs (Waterfield and Zilberman, 2012). Only a small proportion of the pesticides applied to crops actually reaches the target (Pimentel, 2005; van der Werf, 1996). The rest enters the environment, contaminating the air, water, and soil, and often persists for a long period of time. These contaminants threaten terrestrial (e.g., Boatman et al., 2007) and aquatic biodiversity as well as ecosystem functioning (e.g., Beketov et al., 2013), can pose a health risk to farm workers who are not appropriately trained or lack access to protective gear (e.g., Singh and Gupta, 2009), and can cause, e.g., cancer, injury to the nervous system, and lung damage to humans who ingest them (NRC, 1993). In the registration process for new pesticides, manufacturers thus have to prove that persistence in the environment and toxicity to non-target organisms are below specific thresholds, that the pesticide is in fact effective against the target organisms, and that its deliberate release into the environment is warranted.

An integrated assessment of this issue requires extensive data, including information on pesticide use in different cropping systems, the persistence and transport of different pesticides in the soil, changing pest pressure and accompanying changes in pesticide requirements under climate

---

Submitted for review in May 2016 as manuscript number NRES 11931; approved for publication by the Natural Resources & Environmental Systems Community of ASABE in October 2016.

The authors are **Livia Rasche**, Research Associate, Research Unit Sustainability and Global Change, University of Hamburg, Hamburg, Germany, and **Robin A. J. Taylor**, Senior Research Scientist, Blackland Research Center, Texas A&M University, Temple, Texas. **Corresponding author:** Livia Rasche, Universität Hamburg, Grindelberg 5, 20144 Hamburg, Germany; phone: +49-40-42838-7243; e-mail: livia.rasche@uni-hamburg.de.

change, the influence of alternative technologies, such as integrated pest management, on pest pressure, and many more. There may be specific test plots for which all of these data are available, but no such information exists for regional or national scales. To close this information gap, crop models are often used, but no crop model exists that has the capability of simulating many pests for many different crops and simultaneously estimating the amounts of pesticides required to combat them. The pest models that were developed in the past either focused entirely on the spread and growth dynamics of diseases and considered hosts only in a secondary role (see Jones et al., 2010 for a review of these models) or were developed to simulate one specific crop and its diseases, such as the model by Johnson (1992) for potatoes, the model by Buhre et al. (2009) for sugarbeet, the models by Willocquet et al. (2002) and Pinnschmidt et al. (1995) for rice, and the models by Willocquet et al. (2008) and De Wolf et al. (2003) for wheat.

A variety of pests can be simulated for various crops in the CROPGRO model of the cropping system model DSSAT (Jones et al., 2003), and damages can be applied to 23 different crop components. However, daily pest numbers and/or daily pest damage must be provided as input by the user, which also applies to the aforementioned models by Johnson (1992) and Willocquet et al. (2002, 2008). These data are not always available, especially when projecting into the future. Whish et al. (2015) solved this problem for the crop model APSIM (Keating et al., 2003) by linking it to a population cohort modeling framework (DYMEX; Sutherst and Maywald, 1998) in which detailed climate-driven disease and insect models can be realized. This approach is very promising, but the existing models for different insects and diseases are highly sophisticated and time-consuming to develop and thus currently focus mostly on Australia, where the models are mainly developed and applied.

In this study, we therefore developed a generic pest submodel for crop models in order to provide an improved tool for integrated assessments. The submodel was implemented and subsequently tested in the generalized crop model EPIC (Sharpley and Williams, 1990). EPIC was originally designed to assess the effect of soil erosion on soil productivity and is thus composed of physically based components for simulating erosion, plant growth, and all related processes. Due to the many different processes implemented in EPIC, the model can be used to assess the impacts of a wide range of agricultural practices, such as tillage intensities, crop rotations, and the amounts and types of fertilizer used. EPIC's detailed pesticide fate submodel is based on the GLEAMS model (Leonard et al., 1987) in which pesticide transport by runoff, percolate, sediment, and soil evaporation is described through a number of equations. However, pests, which are the causative factors for pesticide applications, are only considered in a very simplified manner. The damage caused by insects and plant diseases is estimated with a pest factor ranging from 0 to 1, which is simulated daily as a function of temperature, rainfall, and crop cover (Williams et al., 2013). The pest factor increases rapidly under high temperatures and rainfall, if crop cover is above a given threshold, and declines when temperatures fall below 0°C. At harvest,

the pest factor is averaged over the time since the last harvest and then multiplied by crop yield to simulate losses due to pests. If a pesticide is applied, which has to be scheduled manually, the accumulated pest factor is reduced by a given pesticide efficiency. This pest function was implemented to rudimentarily simulate the influence of climate on pest occurrences but lacks details, such as the influence of pests on biomass accumulation over the growing season, the possibility of multiple pests with different characteristics occurring simultaneously in a field, the host-pathogen relationship between some pests and crops (which allows crop rotations to ameliorate pest losses), a function for the introduction of new pests to a field, and the possibility of having pesticides applied automatically if the need arises. All of these concerns were addressed in the development of the new pest submodel, which is described in the following sections.

## MATERIAL AND METHODS

### DESCRIPTION OF PEST SUBMODEL

The initial occurrence of pests in a field can be caused by a variety of often random factors, such as infected seeds, infected neighboring fields, or insect vectors carrying a disease. Accurately predicting an initial infection in an agricultural model is therefore very difficult, so instead we decided to randomly introduce pathogens to the field. Before any simulation, the user can input the probability of occurrence ( $po$ ) of a specific disease ( $n$ ) for a specific crop category ( $j$ ). Crop categories in EPIC cover warm and cold season annual legumes, perennial legumes, warm and cold season annuals, perennials, evergreen and deciduous trees, cotton, and N-fixing trees. At the start of each growing season, a random number ( $U$ ) is generated, and an infection occurs if  $po$  is equal to or larger than  $U$ :

$$po_{nj} \geq U \sim U([0,1]) \quad (1)$$

### Insects

Crop pests can be roughly divided into three categories: insects, diseases, and weeds. As soon as insects are introduced to a field, a simple model of insect population growth and feeding rates based on Thornley and France (2007) is activated. In this model, the daily total feeding rate ( $RCON$ ) is described by:

$$RCON = (0.5 \times RRCON) \times IBM_n \times INS \quad (2)$$

where  $RRCON$  is the relative feeding rate,  $IBM_n$  is the biomass of an adult insect, and  $INS$  is the current number of insects per m<sup>2</sup>. It is assumed that insects can consume half of their body weight of plant material per day, hence the 0.5 in equation 2, and that the consumed plant biomass is immediately converted into insect biomass:

$$INS = INS + RCON / IBM_n \quad (3)$$

The daily relative feeding rate ( $RRCON$ ) is a standard biological temperature response function based on the current, optimal, minimum, and maximum temperatures ( $T$ ,  $T_{opt,n}$ ,  $T_{min} = 0^\circ\text{C}$ ,  $T_{max} = 45^\circ\text{C}$ ):

$$RRCON = \frac{(T - T_{min})^2 \times (T_{max} - T)}{(T_{opt,n} - T_{min})^2 \times (T_{max} - T_{opt,n})} \quad (4)$$

for  $T_{min} \leq T \leq T_{max}$ ; otherwise,  $RRCON = 0$

Insects not only increase their numbers, they also suffer mortality. A total mortality rate ( $k_{mort}$ ) is applied daily to the total number of insects:

$$INS_{t+1} = INS_t \times (1 - k_{mort}) \quad (5)$$

where  $k_{mort}$  is calculated by summing nutrient-dependent ( $k_{mort,N}$ ) and temperature-dependent ( $k_{mort,T}$ ) mortality rates and constraining them between maximum and minimum mortality values ( $k_{mort,min} = 0.02$ ,  $k_{mort,max} = 0.1$ ):

$$k_{mort} = \min(\max[k_{mort,min} \cdot (k_{mort,T} + k_{mort,N})], k_{mort,max}) \quad (6)$$

The temperature-dependent mortality rate ( $k_{mort,T}$ ) is described by an inverted parabola:

$$k_{mort,T}(T) = k_{mort,T_0,n} \times \frac{(T - T_{opt,n})^2}{(T_{min} - T_{opt,n})^2} \quad (7)$$

where  $k_{mort,T_0,n}$  is the insect-specific mortality rate at 0°C ( $T_{min}$ ), and  $T_{opt,n}$  is optimal temperature for insect survival, which is assumed to be equal to the optimal temperature for feeding.

The nutrition-dependent mortality rate ( $k_{mort,N}$ ) is described with a “switch-off” sigmoidal response to crop N content ( $UN1$ , kg ha<sup>-1</sup>), where  $q$  (currently set to 1) indicates the steepness of response:

$$k_{mort,N} = k_{mort,N_{max}} \times \frac{K_{N,mort}^q}{K_{N,mort}^q + UN1^q} \quad (8)$$

The maximum mortality rate without food ( $k_{mort,N_{max}}$ ) is 10% per day. Half of the maximum mortality rate occurs when  $UN1 = K_{mort,N} = 50$  kg N ha<sup>-1</sup>.

Low temperatures and missing food thus lead to a high insect mortality, which ensures that fields are usually insect-pest free at the start of each new cropping season. Even though in reality not all insects die in winter (some can enter diapause with anti-freeze to survive), most migrate out and are thus also lost.

Based on Willocquet et al. (2008), the final reduction factor ( $RF$ ) incurred by insect pests is described as:

$$RF_{INS} = \max[1 - (a_1 \times RCON \times a_2), MLD] \quad (9)$$

where  $a_1$  and  $a_2$  are constants used for sap-sucking insects to describe the ratio of sapped phloem that is deposited on the plant as honeydew ( $a_1 = 0.35$ ) and the decreasing rate of CO<sub>2</sub> assimilation, whose minimum is reached 15 days after honeydew deposition ( $a_2 = 0.015$ ).  $MLD$  can be used to cap the maximum level of daily damage ( $MLD = 0.8$ ). To simulate damage to the crop, the reduction factor is multiplied by the value of radiation use efficiency, aboveground plant biomass, leaf area index, or root weight, depending on the com-

partment that the specific pest targets. If an insecticide is applied, the number of insects is decreased based on the efficacy of the pesticide (see “Effects of Insects and Diseases on Crop Growth”).

### Diseases

The progress of disease spread over a plant part was described in a simple model by Gilligan (1974). In this model, the daily increase in the proportion of the diseased to the healthy plant part ( $PDPP$ ) is described by:

$$\frac{dPDPP_j}{dt} = (CPI_n + CSI_n \times PDPP_j) \times (MLI_n - PDPP_j) \quad (10)$$

where  $CPI$  and  $CSI$  are the coefficients of primary and secondary infection, and  $MLI$  is the maximum level of infection of disease  $n$ . The value of  $CPI$  can be calculated by multiplying the current amount of inoculum ( $INOC_{j,n}$ ) with a factor describing the efficiency of the inoculum in causing disease ( $DEIP$ ):

$$CPI_n = INOC_{j,n} \times DEIP_n \quad (11)$$

The value of  $CSI$  in turn is calculated by multiplying the current host density ( $N$ ) with a factor describing the efficiency of the inoculum in causing secondary infections in other parts of the plant ( $DEIS$ ):

$$CSI_n = N_j \times DEIS_n \quad (12)$$

Both host density and inoculum vary with time. Host density ( $N$ ) is calculated in the main EPIC crop growth model. The daily increase in inoculum is calculated using an adapted version of a model described by Thornley and France (2007):

$$INOC_{j,n,t+1} = INOC_{j,n,t} + (INOC_{j,n,t} \times \min[f_T, f_{RH}]) \quad (13)$$

where  $f_T$  and  $f_{RH}$  are functions depending on temperature and relative humidity, respectively;  $f_T$  can be written as:

$$f_T = \max \left[ 0, \min \left[ 1, \frac{T - T_{min}}{T_{opt1} - T_{min}} \right] \right] \times \max \left[ 0, \min \left[ 1, \frac{T_{max} - T}{T_{max} - T_{opt2}} \right] \right] \quad (14)$$

For simplicity's sake, it was assumed that  $T_{min}$ ,  $T_{max}$ ,  $T_{opt1}$ , and  $T_{opt2}$  can all be derived from one disease-specific parameter for optimal temperature ( $FUTO$ ), with  $T_{min} = FUTO_n - 17^\circ\text{C}$ ,  $T_{max} = FUTO_n + 6^\circ\text{C}$ ,  $T_{opt1} = FUTO_n - 2^\circ\text{C}$ , and  $T_{opt2} = FUTO_n + 2^\circ\text{C}$ .

The value of  $f_{RH}$  also varies between 0 and 1 but only takes values above 0 if the current relative humidity is higher than a disease-specific threshold humidity ( $FUHO$ ):

$$f_{RH} = \max \left[ 0, 1 - \left( \frac{1 - RH}{1 - FUHO_n} \right)^2 \right] \quad (15)$$

Lastly, a disease-specific daily inoculum background decay rate ( $DRI$ ) is used to steadily decrease the inoculum:

$$INOC_{j,n,t+1} = INOC_{j,n,t} \times e^{(1-e^{-DRI_n})} \quad (16)$$

Based on the models described by Johnson (1992) and Willocquet et al. (2002, 2008), the final reduction factors are calculated with two different equations, depending on the specific disease:

$$RF_n = (1 - PDPP_j)^{MODU_n} \quad (17)$$

$$RF_n = 1 - (MODU_n \times PDPP_j / 100) \quad (18)$$

Equation 17 is used for spot, rust, blight, blotch, and mildew diseases, and equation 18 is used for take-all, stem rot, and head blight. *MODU* is a disease-specific modifier. The values of all disease-specific parameters used in the simulations are listed in table 1. As with insect pests, to simulate damage to the crop, the reduction factor is multiplied by the value of radiation use efficiency, aboveground plant biomass, leaf area index, or root weight, depending on the compartment that the specific pest targets. If a fungicide is applied, the amount of inoculum is decreased based on the efficacy of the pesticide (see “Effects of Insects and Diseases on Crop Growth”).

#### Effects of Insects and Diseases on Crop Growth

Depending on the specific disease or insect pest, different plant state variables are impacted when an infestation occurs. In EPIC, we distinguish between damages to radiation use efficiency, aboveground plant biomass, leaf area index, and root weight (fig. 1). If more than one active pest is affecting the same compartment on a day, the most severe reduction factor is applied. If the automatic pesticide application function is engaged, an insecticide or fungicide is applied when the total pest stress rises above a user-defined threshold. The pesticides used in the automatic option can be chosen from a pesticide input file. In this file, variables describing the environmental fate of the pesticide are stored in addition to data on recommended dose, minimum number of days between applications, and maximum amount per year. The latter data were taken from the U.S. Environmental Protection Agency (USEPA) pesticide product label system ([www2.epa.gov/pesticides](http://www2.epa.gov/pesticides)). Also recorded in the file is the efficacy of the pesticide, described by dose at 50% and dose

at 90% efficacy, taken from the USEPA ECOTOX database (USEPA, 2015). From these two values, a sigmoidal response curve is calculated based on a function already implemented in EPIC in which an exponential equation is solved based on and passing through the two points, originating at 0 and approaching 1 (Williams et al., 2013, p. 46). The producer-recommended single dose usually approaches maximum efficacy, but manually input pesticide applications, or applications that surpass the allowed maximum annual dose, may have lower efficacy.

#### Weeds

EPIC does not consider natural grassland dynamics, which is why weeds need to be grown like normal crops in the model. We automated this process and established that weeds are planted alongside crops if the number of seeds in the seed bank is above zero. The characteristics of the weed can be specified in the crop parameter input file. The initial value of seeds in the seed bank (SEBA, seeds m<sup>-2</sup>), average seed half-life in the soil (SEDE, days), average 100-seed mass (SEMA, mg), and annual seed bank germination rate (SGERM, %) can be set in the input file describing each site. At planting, the specified percentage of seeds in the seed bank is set to germinate. At harvest, first a potential seed bank increase is calculated based on the total weed biomass and harvest index (describing the actual yield), divided by the seed mass, thus giving the potential number of seeds returning to the seed bank, which in a second step is decreased by a specific percentage representing predation (currently set to 60%). In addition to seed predation, the number of seeds in the seed bank decays continuously based on seed half-life. Tillage also influences weed incidence, as seedling emergence usually decreases with burial depth (Colbach et al., 2000). Because we do not track the depths of seeds, we did not include this feature. However, tillage reduces the standing live biomass of weeds in the model, the intensity of which depends on the mixing efficiency of the equipment used, which can be specified in the EPIC tillage input file.

In EPIC, weeds use the same resources as crops and thus influence either crop growth or input requirements. If the automatic pesticide application function is engaged, a herbicide is applied, targeting weed biomass, each time the weed

**Table 1.** Pest submodel parameters for different diseases and insect pests. Values for *MODU* and *MLI* were taken from Willocquet et al. (2002, 2008), values for *k<sub>mort,70</sub>* were taken from Thornley and France (2007), values for *T<sub>opt</sub>*, *FUHO*, and *IBM* were approximated from different values reported in the literature, and tentative generic values were used for *DEIP*, *DEIS*, and *DRI* due to a lack of more specific data.

		<i>DEIP</i>	<i>DEIS</i>	<i>T<sub>opt</sub></i> (°C)	<i>DRI</i>	<i>MODU</i>	<i>MLI</i>	<i>FUHO</i> (%)	Damage <sup>[a]</sup>
Diseases	Bacterial leaf blight	1e-05	1e-05	29.5	-0.005	1	0.9	0.7	LAI
	Brown rust	1e-05	1e-05	17.5	-0.005	1	0.9	0.75	LAI
	Brown spot	1e-05	1e-05	26	-0.005	6.3	0.9	0.9	LAI
	Fusarium head blight	1e-05	1e-05	27	-0.005	1.1	0.9	0.9	BIOM
	Fusarium stem rot	1e-05	1e-05	27	-0.005	0.93	0.9	0.9	RUE
	Powdery mildew	1e-05	1e-05	18.5	-0.005	2.5	0.9	0.95	LAI
	Take-all	1e-05	1e-05	16	-0.005	1	0.9	0.5	RUE
	<i>Septorium nodorum</i> blotch	1e-05	1e-05	18	-0.005	1	0.9	0.9	LAI
	<i>Septorium tritici</i> blotch	1e-05	1e-05	20	-0.005	1.25	0.9	0.9	LAI
	Sheath blight	1e-05	1e-05	16.5	-0.005	1	0.9	0.92	RW
	Yellow rust	1e-05	1e-05	12.5	-0.005	1.5	0.9	0.5	LAI
Insects				<i>k<sub>mort,70</sub></i>				<i>IBM</i> (mg)	
	Aphids	-	-	27.5	0.04	1	-	3.05	RUE
	Cotton bollworm	-	-	27.5	0.06	1	-	31.3	BIOM
	Thrips	-	-	26	0.04	1	-	1	RUE
	Tobacco budworm	-	-	25	0.04	1	-	140	BIOM

<sup>[a]</sup> LAI = leaf area index, BIOM = aboveground biomass, RUE = radiation use efficiency, and RW = root weight.

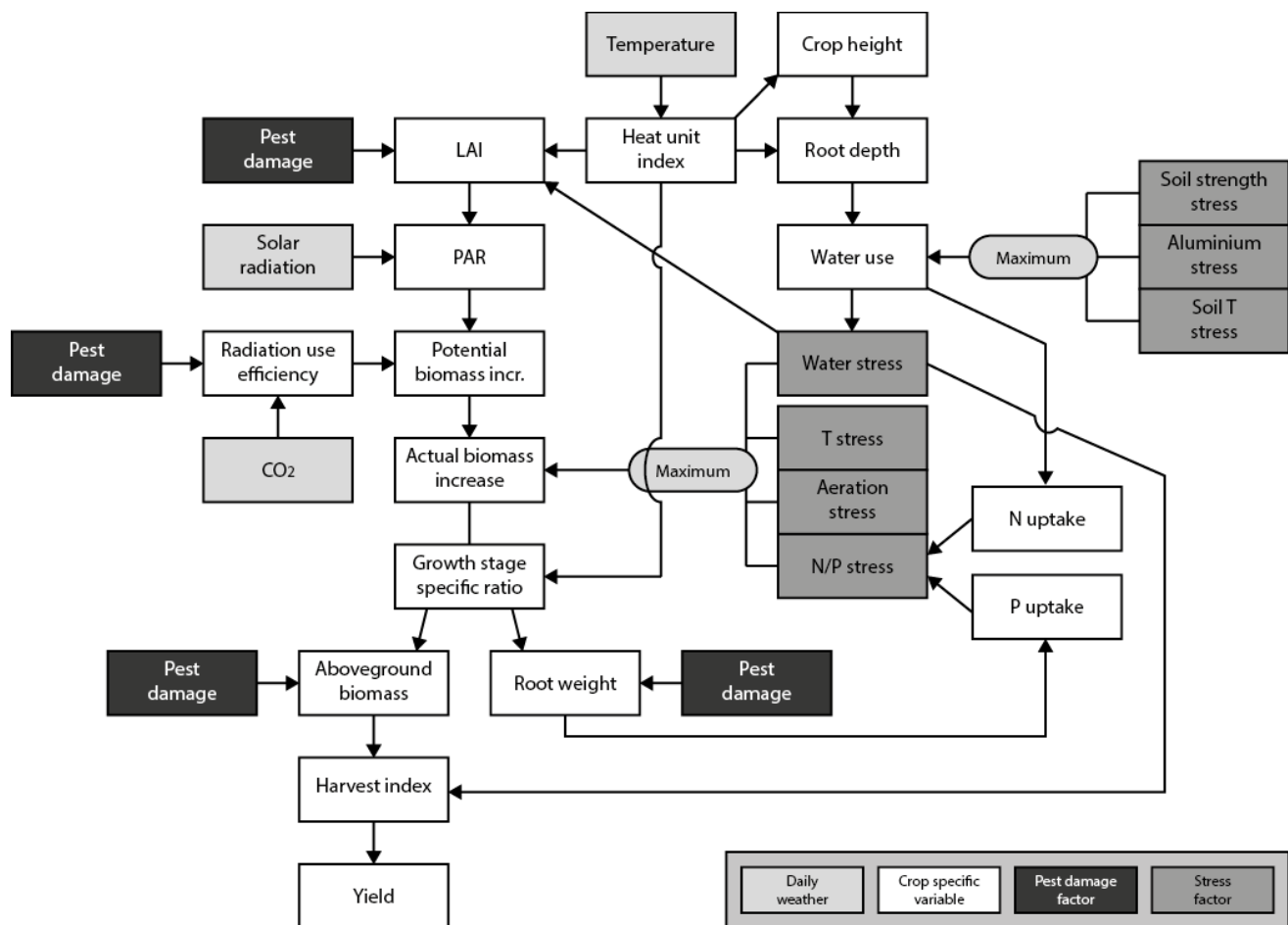


Figure 1. Diagram of crop growth and yield determination in EPIC. A daily potential biomass increase is calculated based on the photosynthetically active part (PAR) of intercepted solar radiation and a species-specific radiation use efficiency, which is affected by atmospheric CO<sub>2</sub> concentration and vapor pressure deficit (Stöckle et al., 1992). This potential biomass increase is then decreased based on water, temperature, nutrient, and aeration stress indices. Similarly, soil strength, temperature, and aluminum toxicity stress indices affect root growth, and thus water use. Aboveground biomass and a harvest index, which can be reduced by water stress, determine the yield. Dark gray boxes point to the crop variables that can be influenced by pests and diseases.

LAI reaches a user-defined proportion of crop LAI. If a pre-emergent herbicide is applied manually (this cannot be triggered automatically by stress), then the number of seeds in the seed bank is reduced. Dose and efficacy are calculated as described in the previous section.

#### INCORPORATION OF SUBMODEL IN EPIC

If the pest submodel is activated, then all relevant input data are read in at the beginning of each simulation. If the seed bank contains seeds, then operations for planting and harvesting of weeds are added to the operations schedule. In the daily simulation loop, a subroutine (PEST) is called that simulates the daily background decay and mortality of pathogens and insects currently present in the field. Once a crop is planted, two things happen: (1) based on the probability of occurrence specified by the user, it is determined if an infection starts for each pest, and (2) in the EPIC subroutine for estimating plant stresses, another subroutine (PSTRS) is called. In this subroutine, the daily increase in inoculum or insect numbers is calculated based on the specific equations, and the spread of disease over the plant parts is updated. If the stress placed on the plant is higher than the stress trigger defined by the user, the pesticide application routine is

called, passing along information if an insecticide, fungicide, or herbicide is needed. By calling the decay function every day for every pest, but calling the growth function only as long as the host crop is growing and only for the pests preying on the current crop group, we ensured that crop rotation can influence the severity of pest stress.

#### TESTING AND VALIDATION SIMULATIONS

For testing purposes, we chose the conterminous U.S., as EPIC was originally developed for this region and has been shown to work well there (e.g., Secchi et al., 2009; Wang et al., 2005), thus minimizing the chances of additional confounding factors. Single simulation units (SimU) for the U.S. were derived by calculating the dominant altitude, soil, and slope class of 5' grid cells (Skalský et al., 2008). The elevation and slope steepness for each cell were derived from the GTOPO30 dataset (30" resolution), climate data (long-term monthly mean temperature, precipitation, radiation, and relative humidity) were provided by the Tyndall Centre for Climate Change Research at 0.5° resolution (Hijmans et al., 2005), and soil data were taken from the Digital Soil Map of the World (1:5,000,000 scale) and the 5' resolution ISRIC-WISE dataset (Batjes, 2012).

Each of the simulation units was then simulated for 50 years, from 1960 to 2010, under three different management systems: high input/irrigated, high input/rainfed, and low input/rainfed. Based on agricultural statistics and land cover data taken from FAOSTAT, AQUASTAT, the International Fertilizer Industry Association, and the USDA, the share of each management system was determined for every SimU. In a last step, the final values of the output parameters for each SimU were calculated as the weighted means of the three management system simulations. We focused mainly on the five crops with the highest rates of pesticide applications in the U.S.: cotton, maize, potatoes, soybeans, and winter wheat. The pest function was initialized in all simulations with default values of 500 seeds  $m^{-2}$  in the seed bank, 1000 days of seed half-life, a 100-seed weight of 303 mg, and a 50% germination rate. If applicable to the specific crop group, the probability of occurrence of a pest was set to 3% to 20% (table 2). These values were determined in a calibration procedure in which we iteratively changed the values based on the match between simulated and reported crop yields, pesticide application rates, and the share of each pesticide type.

For stress-triggered automatic pesticide applications, the pesticides to be used were set to a chlorothalonil fungicide (single dose: 1.16 kg AI  $ha^{-1}$ ; maximum annual dose: 10.08 kg AI  $ha^{-1}$ ; minimum interval: 10 days), a glyphosate herbicide (single dose: 0.42 kg AI  $ha^{-1}$ ; maximum annual dose: 2.63 kg AI  $ha^{-1}$ ; minimum interval: 30 days), and a chlorpyrifos insecticide (single dose: 0.9 kg AI  $ha^{-1}$ ; maximum annual dose: 3.36 kg AI  $ha^{-1}$ ; minimum interval: 10 days) on all sites (Fernandez-Cornejo et al., 2014). The stress triggers were both set to 0.8, meaning that the automatic pesticide application function was called each time radiation use efficiency, biomass, leaf area index, or root weight were reduced by 20% or more due to insect or disease damage, or if the ratio of weed to crop LAI rose above this value. This value was chosen under the assumption that it corresponds to a threshold at which damage is easily observed in the field but not yet severe. Single application rates were set to the producer-recommended values listed above. If the maximum annual application rates for each pesticide type were reached, no more applications were allowed.

After finishing the simulations, we compared the simulated and reported data on yield (FAOSTAT; <http://fao-stat3.fao.org/home/E>) and pesticide use (Fernandez-Cornejo et al., 2014; Thelin and Stone, 2013) and plotted maps of pesticide use and the number of stress days in order to test and validate the submodel. In addition, we ran simulations for all five crops, growing them once as a monoculture and once in rotation with a crop of a different EPIC crop group. We did not apply any pesticides in these simulations in order to test the ability of the submodel to represent the disease-mitigating effects of crop rotation.

## RESULTS AND DISCUSSION

Figure 2a shows the reported yields and yields simulated with and without pesticide applications. A comparison of yields simulated in the conventional setting, i.e., with pesticide applications engaged, and reported yields shows that the submodel underestimated yields for potatoes and, to a lesser degree, maize, whereas cotton, soybean, and wheat yields are adequately represented. This result indicates that simulated pest stresses, and thus the triggered pesticide applications, approximate real-world conditions. A comparison of the two simulated yields (with and without pesticide applications) shows that, with the exception of cotton, yields are significantly lower ( $p \leq 0.03$ ) when no pesticide applications are allowed. Simulated yield losses range from up to 15% for cotton, 27% for maize, 53% for potatoes, 43% for soybeans, and 19% for wheat, which correspond adequately to reported losses of 25% to 49% for cotton, 30% to 60% for maize, up to 75% for potatoes, 24% to 51% for soybeans, and 7% to 34% for wheat (Popp et al., 2013; Taylor et al., 1990), even though some losses are underestimated. The results also suggest that the dose-response curves that we calculated for the pesticides are accurate.

The respective amounts of pesticides applied per hectare are shown in figure 2b. For cotton, maize, and potatoes, the submodel underestimated the mean amount by 3.87, 1.39, and 3.43 kg  $ha^{-1}$ , respectively. For soybeans and wheat, the amount was slightly overestimated by 0.2 and 1.2 kg  $ha^{-1}$ , respectively. Even though the agreement between the reported and simulated amounts is thus not perfect, we deem

**Table 2. Annual probability of occurrence ( $p_o$ ) of each pest for each EPIC crop group.**

		Crop Group <sup>[a]</sup>									
		1	2	3	4	5	6	7 <sup>[b]</sup>	8 <sup>[b]</sup>	9	10 <sup>[b]</sup>
Diseases	Bacterial leaf blight	0	0	0	0	0.08	0.03	0	0	0	0
	Brown rust	0	0	0	0	0.08	0.03	0	0	0	0
	Brown spot	0	0.03	0.03	0	0.08	0.03	0	0	0	0
	Fusarium head blight	0	0	0	0	0.08	0.03	0	0	0	0
	Fusarium stem rot	0	0.03	0.03	0	0	0	0	0	0	0
	Powdery mildew	0	0.03	0.03	0	0.08	0.03	0	0	0	0
	Take-all	0	0	0	0.03	0.08	0.03	0	0	0	0
	<i>Septorium nodorum</i> blotch	0	0	0	0	0.08	0.03	0	0	0	0
	<i>Septorium tritici</i> blotch	0	0	0	0	0.08	0.03	0	0	0	0
	Sheath blight	0	0	0	0	0.08	0.03	0	0	0	0
	Yellow rust	0	0	0	0	0.08	0.03	0	0	0	0
Insects	Aphids	0.04	0.03	0.03	0	0.04	0.03	0	0	0	0
	Cotton bollworm	0.04	0.03	0.03	0	0	0	0	0	0.2	0
	Thrips	0.04	0.03	0.03	0	0.04	0.03	0	0	0.2	0
	Tobacco budworm	0.04	0.03	0.03	0	0	0	0	0	0.2	0

<sup>[a]</sup> 1 and 2 = warm and cold season annual legumes, 3 = perennial legumes, 4 and 5 = warm and cold season annuals, 6 = perennials, 7 and 8 = evergreen and deciduous trees, 9 = cotton, and 10 = N-fixing trees.

<sup>[b]</sup> No crops from these groups were included in our simulations.

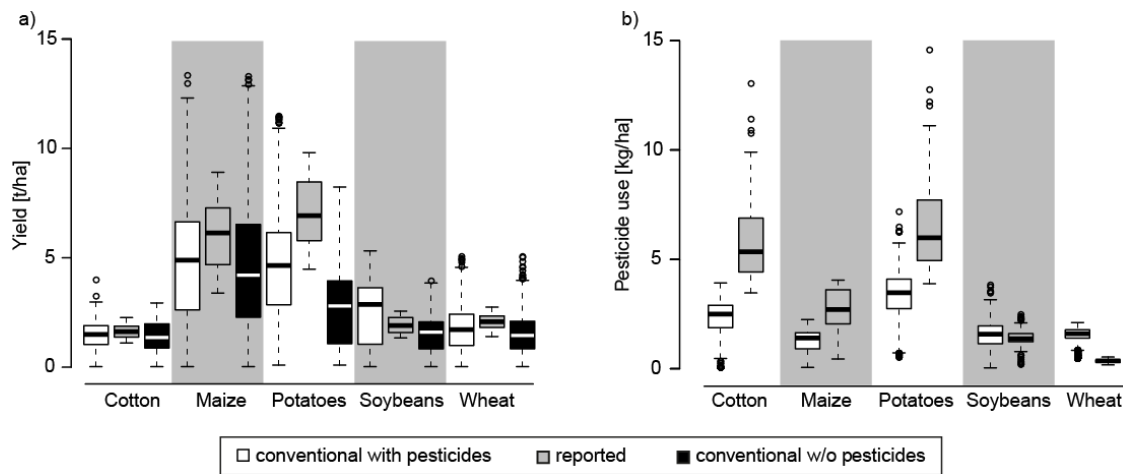


**Figure 2.** Simulated and reported (a) yields and (b) pesticide use in the U.S. Reported yields (annual values from 1960-2010) were taken from the FAOSTAT database, and reported pesticide use (annual values per county, 1992-2009) were taken from Thelin and Stone (2013). Simulation results (annual values per simulation unit) were limited to the corresponding years.

the results satisfactory, as the overestimations for soybeans and wheat are not high and the underestimations are easily explained by several facts. First, in the stress-triggered automatic pesticide application function, only one pesticide can be selected per category for application, and the maximum amount is constrained by producer recommendations. In practice, it is common to apply more than one pesticide to the same crop, and the total amount can consequently be higher. Second, it is common in no-till fields to apply a pre-plant “burn-down” to kill weeds and/or a pre-emergent herbicide, and some crops (especially cotton and potatoes) are desiccated pre-harvest. Neither of these applications is triggered by pest stress, and they are not included in the simulations. When we repeated the simulations for maize with a manually scheduled pre-emergent herbicide application, the mean pesticide application rates were underestimated by only  $0.69 \text{ kg ha}^{-1}$  instead of  $1.39 \text{ kg ha}^{-1}$  (not shown). Third, in the case of cotton, a defoliant is applied to the crop pre-harvest, which can amount to an additional 1 kg of pesticide per hectare. These factors should thus be kept in mind when the submodel is used to generate datasets for use in integrated assessments. Another factor to consider is that it is very difficult to identify exactly how much pesticide is applied to crops, as pesticide producers do not publish sales figures and growers often underreport their application rates for legal reasons.

Figure 3 shows the share of each type of pesticide applied to the five crops. The simulated and reported ratios agree well for cotton and maize. In the case of potatoes, the simulated share of herbicides was overestimated by 36%, and the share of fungicides was underestimated by 29%. For soybeans and wheat, the dominant pesticide (herbicide) was correctly simulated but was underestimated by 12% for soybeans and overestimated by 12% for wheat. The lower right panel shows the total share of each pesticide aggregated over all five crops. Here the agreement is nearly perfect, with the simulated share of herbicides overestimated and the share of fungicides underestimated by only 2% each. These numbers show that even though there is room for improvement, general patterns can be reproduced accurately, and the overall

performance of the submodel is satisfactory. Further interpretation of the results suggests that the simulated occurrences of the different pest categories on the sites are more or less in agreement with the observed incidences. However, this interpretation comes with a caveat, as the decision to apply pesticides depends not only on a pest being observed but also on economic considerations. For example, no insecticide may be applied if an infestation is minimal, or the severity of an infestation may be overestimated and more pesticide applied than necessary. It should also be kept in mind that we only compared ratios of one class each of herbicides, insecticides, and fungicides. There are other classes and groups of pesticides that we did not consider.

For the optimization of land use, it is important that not only mean values are reproduced in agreement with observations, but spatial patterns as well. We thus compared simulated and reported pesticide application intensities across the conterminous U.S. (fig. 4). For this map, we included not only the five crops shown before but also other common crops in the U.S., i.e., barley, beans, flax, groundnuts, pearl millet, peas, rice, sorghum, sugarbeet, sugarcane, sunflowers, and sweet potatoes. Due to the limits of the submodel, vegetables such as salad greens and cucumbers, as well as fruits, were not included, which should be kept in mind when comparing the two maps, especially California and Florida, as the map of reported values includes these categories. The maps show that the intensities broadly agree. Intensities are highest in the Corn Belt, where 80% of farmland is devoted to maize-soybean rotations with an occasional wheat crop and where glyphosate and glufosinate are applied multiple times during the growing season. Intensities are also high in the Mississippi River region and in parts of Idaho, Texas, Louisiana, Florida, and the Atlantic coast states, followed by slightly lower intensities in the northwest and California and relatively low values outside of these regions. The high pesticide intensities reported for large parts of the Pacific coast states and for most of Florida, which the simulations did not reproduce well, can be explained by the aforementioned difference in the crops that we considered.

The factor triggering pesticide applications is the level of



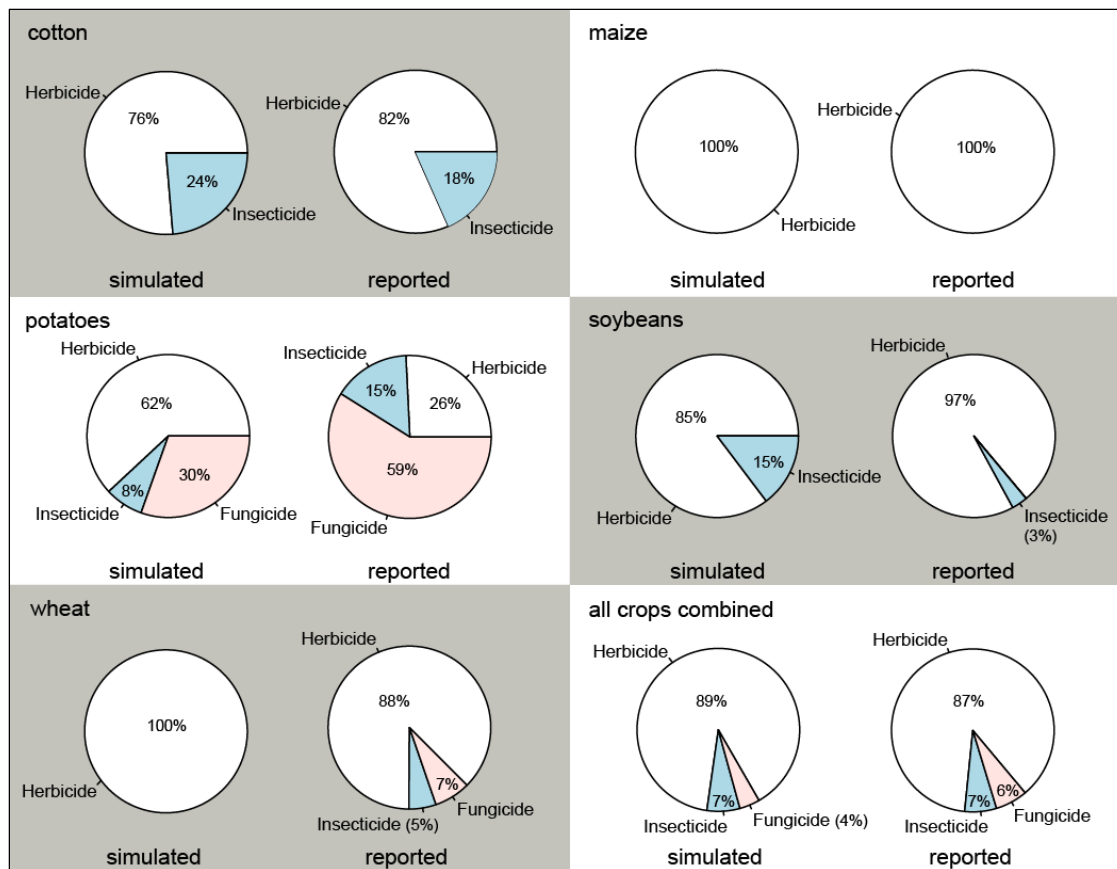


**Figure 3. Simulated and reported shares of each pesticide type applied to cotton, maize, potatoes, soybeans, and wheat and an aggregation of all five crops. Reported shares were taken from Fernandez-Cornejo et al. (2014) but limited to the categories herbicide, insecticide, and fungicide.**

stress that a crop is subjected to by weeds, insect pests, or diseases. To illustrate the spatial distribution of stress levels, we plotted the mean annual stress days triggered by insects or diseases for each crop (fig. 5). Maize and wheat were least stressed by insects and diseases, while soybeans were slightly more stressed. Cotton and potatoes were stressed the most. Whether or not a crop is stressed by insects or diseases is initially dependent on the user-specified pest occurrence probability. These probabilities were set to 0 for most parameterized diseases of wheat and maize (table 2), so the low level of stress is no surprise. Wheat and maize were instead more stressed by competition with weeds. In the case of potatoes, the most stressed crop, the probabilities were set to higher values, which is reflected in the overall higher number of stress days. The spatial heterogeneity of stress days for potatoes and, to a lesser degree, cotton, further shows that the submodel is able to depict the influence of different climatic conditions (temperature and humidity) on the severity of infestation.

Lastly, we tested the submodel's ability to mimic the effects that crop rotations can have on the prevalence of infestations (e.g., Buhre et al., 2009; Larkin et al., 2012; Paulitz et al., 2002; Peters et al., 2003). For this, we chose maize as an example and simulated its cultivation (without pesticide applications) once in perpetual monoculture and once in rotation with a crop not belonging to the same EPIC crop group, which was chosen randomly from a list of crops grown in the same location. Figure 6a shows that the yields

of maize grown in rotation were higher than those of maize grown in monoculture, with an average of 4.6 t ha<sup>-1</sup> for the former and 2.7 t ha<sup>-1</sup> for the latter. The underlying mechanism is shown in figure 6b, where the amount of inoculum over two years' time in a rotation and in a monoculture is plotted for one randomly chosen site. In both cases, an infestation occurred in year 1 and spread over the course of the growing season. In the rotation scenario, a crop of a different crop group was grown in year 2, and the amount of the inoculum slowly degraded in the absence of its host. In the monoculture scenario, the same host returned in the second year, facilitating a steep increase in pathogen numbers and higher crop damage. Figure 6c shows the number of insects on the same plot, also for both scenarios. Insect numbers decline rapidly due to mortality and migration once the cropping season is over, so there is no carry-over between years, and even a return of the same host does not promote a new infestation. In addition, a boost in maize productivity is common when maize follows a nitrogen-fixing crop like soybeans. To achieve a similar level of productivity in continuous maize, large applications of nitrogen are required every year.

Overall, the results showed that the new submodel performed well, but there is room for improvement. As stated above, the submodel is currently set up so that all crops of one EPIC crop group are suitable hosts for a pest preying on this crop group. This assumption is simplistic and should only be applied in simulations where the effect of rotation is not a primary concern, as many diseases have more specific



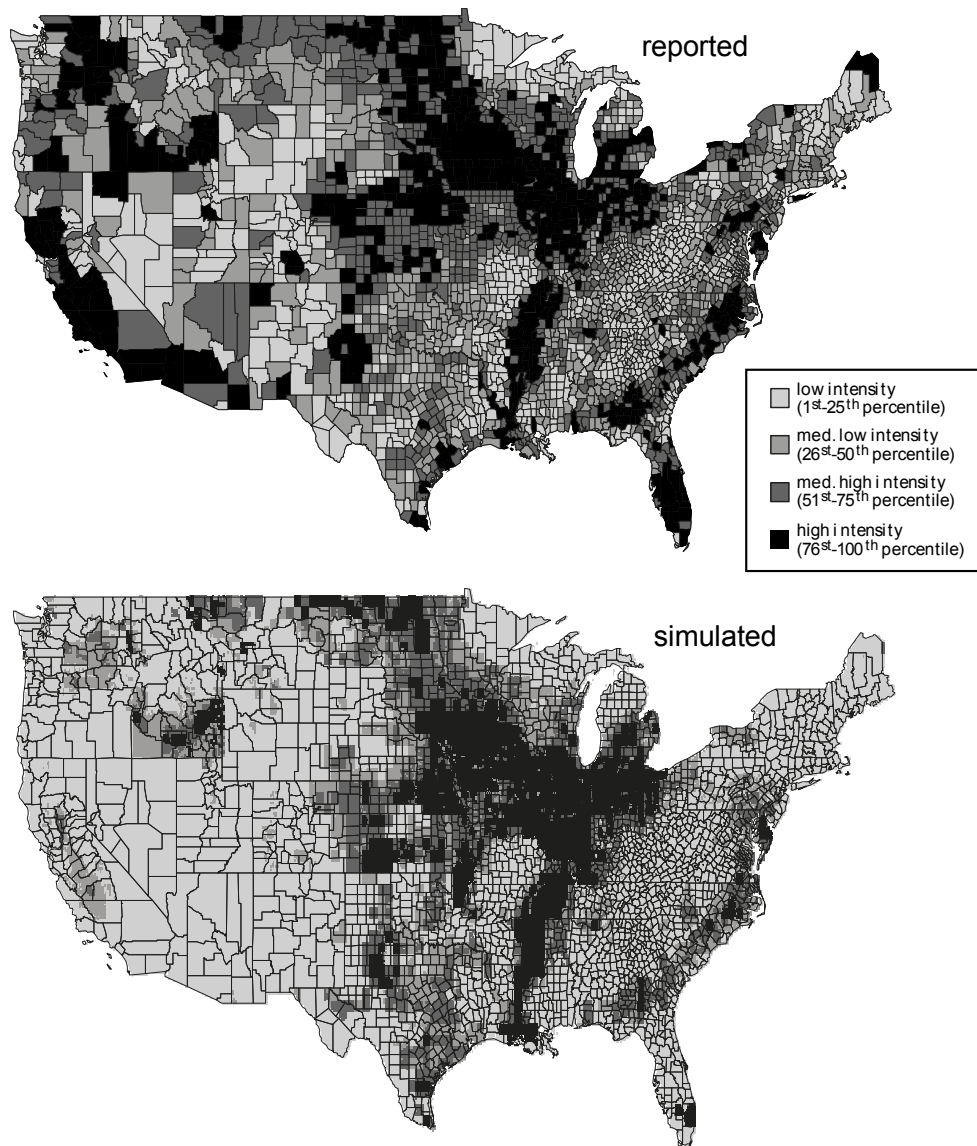


**Figure 4.** Simulated and reported spatial distribution of mean pesticide application intensities. Reported values (total annual amount per county, averaged over 1992–2009) were taken from Thelin and Stone (2013); simulation results (total annual amount per simulation unit) were averaged over all simulation years. To emphasize spatial patterns of pesticide application intensities and facilitate a comparison, we classified both data sets into four classes using the first, second, and third quartiles of the distributions as break points.

hosts. In the future, we plan to move away from the crop-group solution and employ more specific pest groups instead. Other parts of the submodel require further work as well. For example, the insect pest subroutine assumes that all biomass uptake by insects is immediately converted to new insect biomass, which is unrealistic. A more realistic model would include insect development days, which pace the time from egg to adult or from egg to larvae/nymph to pupae to adult, such as described in the NAPPFAST system (e.g., Magarey et al., 2007). Because insects in different development stages may exhibit different susceptibilities to insecticide, this factor can also be taken into account. Lastly, the simulation of competition between weeds and crops needs to be improved, especially for light. The amount of shading and the influence of biomass removal are dependent on the plant geometry and can differ widely, e.g., between plants with a cone-shaped geometry and plants with a reverse cone-shaped geometry. However, this problem is not

unique to EPIC, as many crop models do not consider plant geometry and solely rely on LAI and crop height. Once these adjustments have been made, we plan to test the applicability of the submodel to smaller scales and compare the simulation results to data from field trials.

## SUMMARY AND CONCLUSIONS

In this article, we described the development and testing of a generic pest submodel for use in large-scale applications and implemented in the crop model EPIC. The submodel provides estimates of pesticide use based on pest pressure and the corresponding damages to crop biomass and yield. Based on well-known principles, a plant disease occurs in the model when an effective pathogen encounters a susceptible host and environmental conditions are suitable, and farmers can influence host susceptibility by applying pesti-

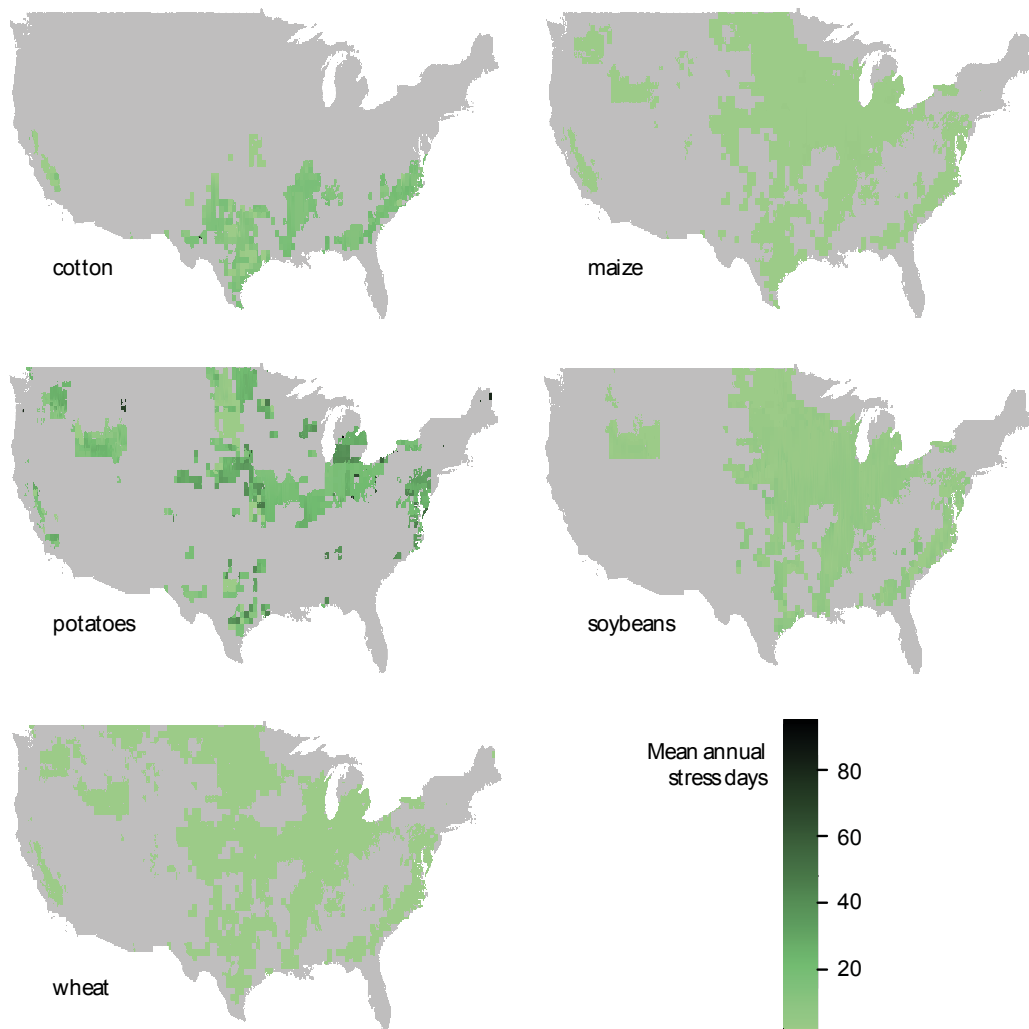


Figure 5. Spatial distribution of simulated mean annual number of days on which crops are stressed by insect pests or diseases when no pesticides are applied. A day is counted as a stress day if at least one of the four compartments (aboveground biomass, leaf area index, radiation use efficiency, or root weight) is damaged by either insects or disease.

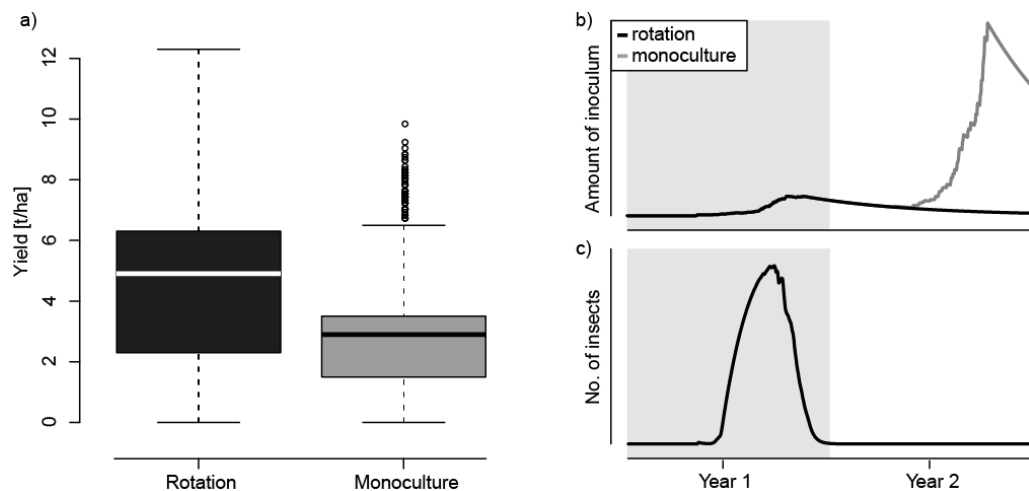


Figure 6. Comparison of (a) simulated maize yield grown once in a rotation system with crops of a different EPIC crop group (black) and in monoculture (gray) covering the years 1960-2010 and all simulation units grown with maize in the U.S. One of these simulation units was randomly chosen to show (b) the amount of inoculum and (c) the number of insects over two years' time, again for maize grown in rotation and monoculture. In (c) the gray line is covered entirely by the black line.

cides and reduce inoculum by crop rotation (West et al., 2012). We tested the submodel by simulating the five most pesticide-intensive non-fruit or vegetable crops in the U.S. (cotton, maize, potatoes, soybeans, wheat) and compared yields, pesticide use (aggregated and spatially explicit), and the share of the different pesticide types against empirical data. Even though many results were satisfactory, other results indicated that further refinements and more details are needed in some of the subroutines. In general, however, the new submodel performed acceptably, especially for our stated purpose of large-scale simulations in connection to integrated assessment.

## ACKNOWLEDGEMENT

This material is based upon work partially supported by the Natural Resources Conservation Service, U.S. Department of Agriculture, under Agreement #68-7482-16-522. Any opinions, findings, conclusions, or recommendations expressed in this publication are those of the authors and do not necessarily reflect the views of the U.S. Department of Agriculture. USDA is an equal opportunity provider and employer.

## REFERENCES

- Batjes, N. H. (2012). ISRIC-WISE derived soil properties on a 5 by 5 arc-minutes global grid (ver. 1.2). Wageningen, The Netherlands: ISRIC. Retrieved from [http://www.isric.org/sites/default/files/isric\\_report\\_2012\\_01.pdf](http://www.isric.org/sites/default/files/isric_report_2012_01.pdf)
- Beketov, M. A., Kefford, B. J., Schafer, R. B., & Liess, M. (2013). Pesticides reduce regional biodiversity of stream invertebrates. *Proc. Natl. Acad. Sci.*, 110(27), 11039-11043. <http://dx.doi.org/10.1073/pnas.1305618110>
- Boatman, N. D., Parry, H. R., Bishop, J. D., & Cuthbertson, A. G. S. (2007). Impacts of agricultural change on farmland biodiversity in the U. K. In R. E. Hester, & R. M. Harrison (Eds.), *Biodiversity under threat* (Vol. 25, pp. 1-32). Cambridge, UK: Royal Society of Chemistry.
- Buhre, C., Kluth, C., Burcky, K., Marlander, B., & Varrelmann, M. (2009). Integrated control of root and crown rot in sugar beet: Combined effects of cultivar, crop rotation, and soil tillage. *Plant Disease*, 93(2), 155-161. <http://dx.doi.org/10.1094/PDIS-93-2-0155>
- Colbach, N., Roger-Estrade, J., Chauvel, B., & Caneill, J. (2000). Modelling vertical and lateral seed bank movements during mouldboard ploughing. *European J. Agron.*, 13(2-3), 111-124. [http://dx.doi.org/10.1016/S1161-0301\(00\)00069-1](http://dx.doi.org/10.1016/S1161-0301(00)00069-1)
- De Wolf, E. D., Madden, L. V., & Lipps, P. E. (2003). Risk assessment models for wheat *Fusarium* head blight epidemics based on within-season weather data. *Phytopathology*, 93(4), 428-435. <http://dx.doi.org/10.1094/PHYTO.2003.93.4.428>
- Fernandez-Cornejo, J., Nehring, R., Osteen, C., Wechsler, S. J., Martin, A., & Vialou, A. (2014). Pesticide use in U.S. agriculture: 21 selected crops, 1960-2008. Washington, DC: USDA Economic Research Service. Retrieved from [http://www.ers.usda.gov/webdocs/publications/eib124/46734\\_eib124.pdf](http://www.ers.usda.gov/webdocs/publications/eib124/46734_eib124.pdf)
- Foley, J. A., Ramankutty, N., Brauman, K. A., Cassidy, E. S., Gerber, J. S., Johnston, M., ... Zaks, D. P. (2011). Solutions for a cultivated planet. *Nature*, 478(7369), 337-342. <http://dx.doi.org/10.1038/nature10452>
- Gilligan, C. A. (1990). Mathematical modeling and analysis of soilborne pathogens. In J. Kranz (Ed.), *Epidemics of plant diseases: Mathematical analysis and modeling* (pp. 96-142). Heidelberg, Germany: Springer-Verlag. [http://dx.doi.org/10.1007/978-3-642-75398-5\\_4](http://dx.doi.org/10.1007/978-3-642-75398-5_4)
- Hijmans, R. J., Cameron, S. E., Parra, J. L., Jones, P. G., & Jarvis, A. (2005). Very high resolution interpolated climate surfaces for global land areas. *Intl. J. Climatol.*, 25(15), 1965-1978. <http://dx.doi.org/10.1002/joc.1276>
- Johnson, K. B. (1992). Evaluation of a mechanistic model that describes potato crop losses caused by multiple pests. *Phytopathology*, 82(3), 363-369. <http://dx.doi.org/10.1094/Phyto-82-363>
- Jones, J. W., Hoogenboom, G., Porter, C. H., Boote, K. J., Batchelor, W. D., Hunt, L. A., ... Ritchie, J. T. (2003). The DSSAT cropping system model. *European J. Agron.*, 18(3-4), 235-265. [http://dx.doi.org/10.1016/S1161-0301\(02\)00107-7](http://dx.doi.org/10.1016/S1161-0301(02)00107-7)
- Jones, R. A. C., Salam, M. U., Maling, T. J., Diggle, A. J., & Thackray, D. J. (2010). Principles of predicting plant virus disease epidemics. *Annu. Rev. Phytopathol.*, 48(1), 179-203. <http://dx.doi.org/10.1146/annurev-phyto-073009-114444>
- Keating, B. A., Carberry, P. S., Hammer, G. L., Probert, M. E., Robertson, M. J., Holzworth, D., ... Smith, C. J. (2003). An overview of APSIM: A model designed for farming systems simulation. *European J. Agron.*, 18(3-4), 267-288. [http://dx.doi.org/10.1016/S1161-0301\(02\)00108-9](http://dx.doi.org/10.1016/S1161-0301(02)00108-9)
- Larkin, R. P., Honeycutt, C. W., Olanya, O. M., Halloran, J. M., & He, Z. (2012). Impacts of crop rotation and irrigation on soilborne diseases and soil microbial communities. In Z. He, R. P. Larkin, & C. W. Honeycutt (Eds.), *Sustainable potato production: Global case studies* (pp. 23-41). Dordrecht, The Netherlands: Springer. [http://dx.doi.org/10.1007/978-94-007-4104-1\\_2](http://dx.doi.org/10.1007/978-94-007-4104-1_2)
- Leonard, R. A., Knisel, W. G., & Still, D. A. (1987). GLEAMS: Groundwater loading effects of agricultural management systems. *Trans. ASAE*, 30(5), 1403-1418. <http://dx.doi.org/10.13031/2013.30578>
- Magarey, R. D., Fowler, G. A., Borchert, D. M., Sutton, T. B., Colunga-Garcia, M., & Simpson, J. A. (2007). NAPPFAST: An internet system for the weather-based mapping of plant pathogens. *Plant Disease*, 91(4), 336-345. <http://dx.doi.org/10.1094/PDIS-91-4-0336>
- NRC. (1993). Pesticides in the diets of infants and children. Washington, DC: National Research Council.
- Paulitz, T. C., Smiley, R. W., & Cook, R. J. (2002). Insights into the prevalence and management of soilborne cereal pathogens under direct seeding in the Pacific Northwest, U.S. *Canadian J. Plant. Pathol.*, 24(4), 416-428. <http://dx.doi.org/10.1080/07060660209507029>
- Peters, R. D., Sturz, A. V., Carter, M. R., & Sanderson, J. B. (2003). Developing disease-suppressive soils through crop rotation and tillage management practices. *Soil Tillage Res.*, 72(2), 181-192. [http://dx.doi.org/10.1016/S0167-1987\(03\)00087-4](http://dx.doi.org/10.1016/S0167-1987(03)00087-4)
- Pimentel, D. (2005). Environmental and economic costs of the application of pesticides primarily in the United States. *Environ. Dev. Sustain.*, 7(2), 229-252. <http://dx.doi.org/10.1007/s10668-005-7314-2>
- Pinnschmidt, H. O., Batchelor, W. D., & Teng, P. S. (1995). Simulation of multiple-species pest damage in rice using CERES-Rice. *Agric. Syst.*, 48(2), 193-222. [http://dx.doi.org/10.1016/0308-521X\(94\)00012-G](http://dx.doi.org/10.1016/0308-521X(94)00012-G)
- Popp, J., Peto, K., & Nagy, J. (2013). Pesticide productivity and food security: A review. *Agron. Sustain. Dev.*, 33(1), 243-255. <http://dx.doi.org/10.1007/s13593-012-0105-x>
- Secchi, S., Gassman, P. W., Williams, J. R., & Babcock, B. A. (2009). Corn-based ethanol production and environmental quality: A case of Iowa and the Conservation Reserve Program.

- Environ. Mgmt.*, 44(4), 732-744.  
<http://dx.doi.org/10.1007/s00267-009-9365-x>
- Sharpley, A. N., & Williams, J. R. (1990). Erosion productivity impact calculator: 1. Model documentation. Washington, DC: USDA Agricultural Research Service.
- Singh, B., & Gupta, M. K. (2009). Pattern of use of personal protective equipments and measures during application of pesticides by agricultural workers in a rural area of Ahmednagar district, India. *Indian J. Occup. Environ. Med.*, 13(3), 127.  
<http://dx.doi.org/10.4103/0019-5278.58915>
- Skalský, R., Tarasovicová, Z., Balkovič, J., Schmid, E., Fuchs, M., Moltchanova, E., ... Scholtz, P. (2008). GEO-BENE global database for bio-physical modeling v. 1.0: Concepts, methodologies, and data. Laxenburg, Austria: International Institute for Applied Systems Analysis. Retrieved from [http://www.geo-bene.eu/files/Deliverables/Geo-BeneGlbDb10\(DataDescription\).pdf](http://www.geo-bene.eu/files/Deliverables/Geo-BeneGlbDb10(DataDescription).pdf)
- Stöckle, C. O., Williams, J. R., Rosenberg, N. J., & Jones, C. A. (1992). A method for estimating the direct and climatic effects of rising atmospheric carbon dioxide on growth and yield of crops: Part I. Modification of the EPIC model for climate change analysis. *Agric. Syst.*, 38(3), 225-238.  
[http://dx.doi.org/10.1016/0308-521X\(92\)90067-X](http://dx.doi.org/10.1016/0308-521X(92)90067-X)
- Sutherst, R. W., & Maywald, G. F. (1998). DYMEX modelling workshops: A national, collaborative approach to pest risk analysis and IPM in Australia. In M. Zalucki and R. Drew (Eds.), *Pest Management—Future Challenges: Proc. 6th Australasian Appl. Entomol. Res. Conf.* (pp. 57-62). St. Lucia, Queensland, Australia: University of Queensland Press.
- Taylor, C. R., Penson, J. B., Smith, E. G., & Knutson, R. D. (1991). Economic impacts of chemical use reduction on the south. *Southern J. Agric. Econ.*, 13(1), 15-23.
- Thelin, G. P., & Stone, W. W. (2013). Estimation of annual agricultural pesticide use for counties of the conterminous United States, 1992-2009. USGS Scientific Investigation Report 2013-5009. Reston, VA: U.S. Geological Survey.
- Thornley, J. H., & France, J. (2007). *Mathematical models in agriculture: Quantitative methods for the plant, animal, and ecological sciences* (2nd ed.). Wallingford, UK: CABI.
- USEPA. (2015). ECOTOX User Guide: ECOTOXicology Database System. Ver. 4.0. Washington, DC: U.S. Environmental Protection Agency. Retrieved from <http://www.epa.gov/ecotox/>
- van der Werf, H. M. G. (1996). Assessing the impact of pesticides on the environment. *Agric. Ecosyst. Environ.*, 60(2), 81-96.  
[http://dx.doi.org/10.1016/S0167-8809\(96\)01096-1](http://dx.doi.org/10.1016/S0167-8809(96)01096-1)
- van Ittersum, M. K., & Wery, J. (2007). Integrated assessment of agricultural systems at multiple scales. In J. H. J. Spiertz, P. C. Struik, and H. H. van Laar (Eds.), *Scale and complexity in plant systems research: Gene-plant-crop relations* (pp. 303-317). Berlin, Germany: Springer.
- Wang, X., He, X., Williams, J. R., Izaurralde, R. C., & Atwood, J. D. (2005). Sensitivity and uncertainty analyses of crop yields and soil organic carbon simulated with EPIC. *Trans. ASAE*, 48(3), 1041-1054. <http://dx.doi.org/10.13031/2013.18515>
- Waterfield, G., & Zilberman, D. (2012). Pest management in food systems: An economic perspective. *Annu. Rev. Environ. Resour.*, 37(1), 223-245. <http://dx.doi.org/10.1146/annurev-environ-040911-105628>
- West, J. S., Townsend, J. A., Stevens, M., & Fitt, B. D. L. (2012). Comparative biology of different plant pathogens to estimate effects of climate change on crop diseases in Europe. *European J. Plant Pathol.*, 133(1), 315-331.  
<http://dx.doi.org/10.1007/s10658-011-9932-x>
- Whish, J. P., Herrmann, N. I., White, N. A., Moore, A. D., & Kriticos, D. J. (2015). Integrating pest population models with biophysical crop models to better represent the farming system. *Environ. Model. Software*, 72, 418-425.  
<http://dx.doi.org/10.1016/j.envsoft.2014.10.010>
- Williams, J. R., Gerik, T., Francis, L., Greiner, J., Magre, M., Meinardus, A., ... Taylor, R. (2013). Environmental policy integrated climate model. User's manual. Ver. 0810. Temple, TX: Texas A&M AgriLife.
- Willcoquet, L., Aubertot, J. N., Lebard, S., Robert, C., Lannou, C., & Savary, S. (2008). Simulating multiple pest damage in varying winter wheat production situations. *Field Crops Res.*, 107(1), 12-28. <http://dx.doi.org/10.1016/j.fcr.2007.12.013>
- Willcoquet, L., Savary, S., Fernandez, L., Elazegui, F. A., Castilla, N., Zhu, D., ... Srivastava, R. K. (2002). Structure and validation of RICEPEST: A production situation-driven crop growth model simulating rice yield response to multiple pest injuries for tropical Asia. *Ecol. Model.*, 153(3), 247-268.  
[http://dx.doi.org/10.1016/S0304-3800\(02\)00014-5](http://dx.doi.org/10.1016/S0304-3800(02)00014-5)